Available online at www.sciencedirect.com

ScienceDirect

*Mendeleev Commun.*, 2019, **29**, 315–317

Mendeleev Communications

# Geometries and NMR properties of cisplatin and transplatin revisited at the four-component relativistic level

**Valentin A. Semenov, Yury Yu. Rusakov, Dmitry O. Samultsev and Leonid B. Krivdin***

*A. E. Favorsky Irkutsk Institute of Chemistry, Siberian Branch of the Russian Academy of Sciences, 664033 Irkutsk, Russian Federation. E-mail: krivdin_office@irioch.irk.ru*

DOI: 10.1016/j.mencom.2019.05.025

**The equilibrium structures of cisplatin and transplatin were optimized, and their $^{1}$H, $^{15}$N, and $^{195}$Pt NMR chemical shifts were evaluated at both non-relativistic and fully relativistic four-component levels. Reliable correlations with experimental data were achieved at the DFT level with taking into account relativistic effects in calculations of both geometrical parameters and NMR chemical shifts.**


It is very well known that biologically active platinum complexes play an important role in the modern pharmaceutical industry of anticancer, antiviral and antibacterial drugs. Although the process of the activity suppression in cancer cells based on aminoplatinates is extremely efficient, to date, its mechanism is still not completely understood. As a classical example, although cisplatin **1** is one of the leading drugs administered against the cancer, its isomer, transplatin **2**, is not cytotoxic. In line with a general breakthrough in the field of computational NMR,[1–6] recent advances of relativistic approach to calculate NMR properties at the relativistic two- and four-component levels have received a special consideration.[7–12] In this preliminary report, we demonstrate the potential of the fully relativistic four-component Dirac's approach to the structural investigation of cisplatin and transplatin including both geometrical studies and calculation of their $^{1}$H, $^{15}$N, and $^{195}$Pt NMR chemical shifts.


Geometries of compounds **1** and **2** were optimized at both non-relativistic (one-component) and fully relativistic (four-component) levels using classical hybrid and generalized gradient approximation (GGA) functionals: B3LYP as the most common three-parameter hybrid functional of Becke[13] in combination with the correlation functional of Lee, Yang and Parr (LYP);[14] BHLYP–Becke's half and half of HF/DFT hybrid exchange (BH)[15] functionals combined with the LYP correlation functional;[14] OLYP, which is Handy and Cohen's OPTX hybrid functional[16] in combination with the LYP correlation functional;[14] the generalized gradient functional of Perdew, Burke and Ernzerhof (PBE);[17] PBE0, the generalized gradient functional of PBE[17] with a predetermined amount of exact exchange;[18] PBE38, a modification of the PBE0 functional with a fraction of 3/8 (37.5 %) of the Fock-exchange.[19] Moreover, to investigate an effect of the accurate exchange on the optimization of the functional quality exemplified for BHLYP, the inclusion of the exchange part of Becke's functional was varied as 50, 60 and 70%.

The most efficient DFT functional for the equilibrium geometry optimizations of cisplatin was chosen based on the comparison of calculated geometric parameters with the known experimental X-ray data.[20] Herewith, we used the Pt–N bond length as the main conditional criterion for choosing the functional that most accurately describes the equilibrium structure of cisplatin. Geometry optimizations were carried out by a series of calculations using a number of the above mentioned functionals, both at the non-relativistic level and with taking into account relativistic effects at the four-component relativistic level using the all-electron double-zeta dyall.ae2z relativistic basic set (Figure 1 and Table S1, see Online Supplementary Materials).

First of all, these results suggest that the fraction of the exact exchange, exemplified for the BHLYP, B60LYP and B70LYP functionals, has practically no effect on the resulting equilibrium structure of cisplatin. In this case, the normalized mean absolute error (NMAE) for the Pt–N bond length, which was obtained as the ratio of the error in the calculated bond length to its experimental value, was about 17–18% for the non-relativistic calculations and as much as 14–15% upon taking into account the relativistic effects. Much more accurate results were achieved with B3LYP and

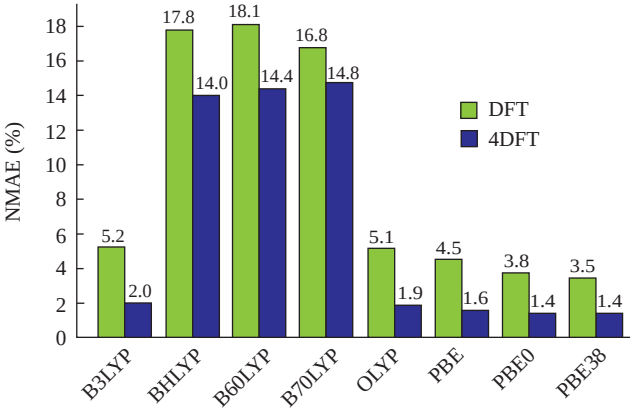


**Figure 1** Normalized mean absolute errors (NMAE) in the calculated Pt–N bond length of cisplatin estimated at the non-relativistic (DFT) and four-component relativistic (4DFT) levels.

OLYP hybrid functionals. In this case, the error was about 5 and 2% for the non-relativistic and relativistic calculations, respectively. However, the most interesting results in this series of geometry optimizations were obtained using the PBE family of functionals. For instance, an increase in the HF exchange fraction from 0 to 38% resulted in the NMAE decrease to 3.5% in the case of the non-relativistic approximation and to as small as 1.4% with taking into account the relativistic effects. Thus, the PBE38 functional was selected as the most reliable one for all the further geometry optimizations of both cisplatin and transplatin.

As a next step of the geometry refinement, the equilibrium structures of cisplatin and transplatin obtained at the full four-component relativistic level within the DFT framework (4c PBE38) were adjusted for the effective geometry evaluated with taking into account zero point vibrational corrections (ZPVC) at the PBE38/ADZP non-relativistic level. However, this aspect of our work will be disclosed in detail in our future reports. In addition, the structures of cisplatin and transplatin, taken in their 'explicit form' based on the related crystallographic experiments, were also used in the calculation of their $^{1}$H, $^{15}$N, and $^{195}$Pt NMR chemical shifts. Tables 1 and 2 contain the $^{1}$H, $^{15}$N and $^{195}$Pt NMR chemical shifts calculated using different combinations of functionals and basis sets, while Table 3 shows these values obtained using experimental X-ray geometries.

Equilibrium geometries of **1** and **2** used for the calculation of chemical shifts were based on three different sources of geometrical data: (i) non-relativistic PBE38/dyall.ae2z optimization, (ii) fully relativistic 4c PBE38/dyall.ae2z optimization, and (iii) experimental X-ray geometries.[20,21] Based on these methods, the $^{1}$H, $^{15}$N and $^{195}$Pt NMR chemical shifts were calculated (see Table 1) for the non-relativistic geometries using the following DFT functionals: two non-parametric gradient functionals (PBE and PBE38) showing the best performance as compared to the experiment and the generalized gradient exchange-correlation functional of Keal and Tozer, KT2,[22] which demonstrated very good efficiency in the calculation of $^{15}$N NMR chemical shifts for a number of nitrogen-containing heterocycles.[3,23] Previously, we used Keal and Tozer's functionals, KT2 and KT3. Both of them proved to be reliable in calculations of chemical shifts. However, the KT2 functional has performed slightly better in our preliminary calculations for these particular compounds **1** and **2**.

**Table 1** NMR chemical shifts of cisplatin and transplatin calculated at the non-relativistic GIAO-DFT/dyall.ae2z//aug-pcS-2 level.[a]

| Compound | Nucleus | PBE | PBE38 | KT2 | Experiment[b] |
|---|---|---|---|---|---|
| **1** | $^{1}$H | 3.08 | 2.57 | 3.06 | 3.93 |
| | $^{15}$N | –396.4 | –411.4 | –400.9 | –424.9 |
| | $^{195}$Pt | –679.1 | –777.1 | –737.4 | –2101.0 |
| **2** | $^{1}$H | 2.51 | 2.17 | 2.51 | 3.60 |
| | $^{15}$N | –396.9 | –411.2 | –402.1 | –425.3 |
| | $^{195}$Pt | –958.8 | –1014.6 | –983.4 | –2104.0 |

[a] Evaluated as $\delta = \delta_{st} + \sigma_{st} - \sigma$; where $\delta$ is the calculated chemical shift, $\delta_{st}$ is the experimental chemical shift of a standard, $\sigma_{st}$ and $\sigma$ are the shielding constants of a standard and an investigated compound, respectively. All the geometries were optimized at the PBE38/dyall.ae2z level. All the calculated and experimental NMR chemical shifts are given in ppm with respect to $SiMe_4$ (for $^{1}$H), nitromethane (for $^{15}$N), and sodium hexachloroplatinate (for $^{195}$Pt). [b] Experimental values were taken from different sources, the references are cited in the main text.

**Table 2** NMR chemical shifts of cisplatin and transplatin calculated at the non-relativistic and four-component KT2/dyall.ae2z//aug-pcS-2 relativistic levels.[a]

| Compound | Nucleus | KT2 | 4c KT2 | Experiment[b] |
|---|---|---|---|---|
| | $^{1}$H | 3.41 | 3.90 | 3.93 |
| **1** | $^{15}$N | –395.7 | –416.2 | –424.9 |
| | $^{195}$Pt | –1220.7 | –2181.2 | –2101.0 |
| | $^{1}$H | 3.11 | 3.25 | 3.60 |
| **2** | $^{15}$N | –417.3 | –431.6 | –425.3 |
| | $^{195}$Pt | –1270.1 | –2606.2 | –2104.0 |

[a,b] See footnotes to Table 1.

**Table 3** NMR chemical shifts of cisplatin and transplatin calculated at the non-relativistic and four-component KT2/dyall.ae2z//aug-pcS-2 level using X-ray geometries.[a]

| Compound | Nucleus | KT2 | 4c KT2 | Experiment[b] |
|---|---|---|---|---|
| **1** | $^{15}$N | –438.3 (13.4)[c] | –434.1 (9.2) | –424.9 |
| | $^{195}$Pt | –1688.2 (–412.8) | –2696.9 (595.9) | –2101.0 |
| **2** | $^{15}$N | –437.3 (12.0) | –434.0 (8.7) | –425.3 |
| | $^{195}$Pt | –2615.2 (511.2) | –2440.0 (336.0) | –2104.0 |

[a,b] See footnotes to Table 1. [c] Given in parentheses are the errors (ppm) of calculated NMR chemical shifts *vs.* the experiment.

To optimize computational costs for the $^{1}$H, $^{15}$N, and $^{195}$Pt NMR chemical shifts, the well-known locally dense basic set (LDBS)[24] scheme was applied. In this way, the platinum atoms were assigned with a full-electron double-splitted Dyall's basis set dyall.ae2z, while Jensen's triple zeta aug-pcS-2 basis set augmented with diffuse functions was used for all N and H atoms. The latter was especially optimized for chemical shift calculations.

Table 1 shows that for the $^{1}$H NMR chemical shifts, the best agreement with experimental values within an error of about 1 ppm was achieved with the PBE and KT2 functionals. In the case of $^{15}$N and $^{195}$Pt NMR shifts, there was also some advantage observed for the PBE38 and KT2 functionals. However, the calculation of chemical shifts in the non-relativistic domain does not allow one to predict the advantage of any of the studied DFT functionals for the investigated platinates, since the relativistic effects of platinum were not taken into account. A fairly considerable disagreement of several hundreds of parts per million was observed for the $^{195}$Pt NMR shifts as compared to the experiment in the case of non-relativistic chemical shifts calculated with the non-relativistic geometric parameters. This situation was essentially improved when both the calculations were performed at fully relativistic four-component level.

The accuracy of the performed calculations was further increased by taking into account the relativistic corrections evaluated at the four-component level with the KT2 functional (4c KT2).

In the agreement with the experimental values, a significant improvement of all NMR chemical shifts of cisplatin and transplatin calculated at the four-component level as compared to the non-relativistic calculations was observed for all three isotopes (Table 2). On the absolute scale, this improvement was found being as much as 0.2–0.5, 8–20 and 800–1000 ppm for the $^{1}$H, $^{15}$N and $^{195}$Pt NMR chemical shifts, respectively.

We have also calculated $^{15}$N and $^{195}$Pt NMR chemical shifts of **1** and **2** using experimental X-ray geometries for the nitrogen and platinum atoms (see Table 3). In this case, the absolute errors are roughly equal to the average values between the geometries in the non-relativistic approximation and the geometries obtained at the four-component relativistic level. This result indicates the well-known fact that the packing of crystals affects the stereoelectronic structure of the investigated complexes by breaking their initial symmetry, which consequently results in the regular deviation from the NMR chemical shifts calculated for the liquid phase.

Figure 2 shows the mean absolute errors (MAE) and their normalized values (NMAE) as compared to the experiment for the $^{15}$N NMR chemical shifts of **1** and **2** evaluated at the non-relativistic one-component and fully relativistic four-component levels using different geometries (*viz.*, those optimized with

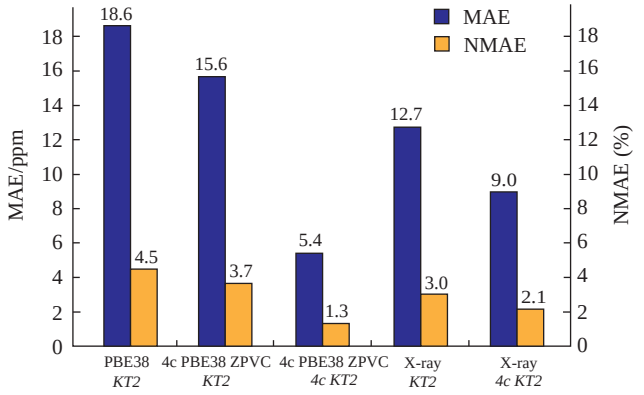


**Figure 2** Mean absolute errors (MAE) and normalized mean absolute errors (NMAE) for the $^{15}$N NMR chemical shifts of compounds **1** and **2** calculated at the one- and four-component KT2 levels (KT2 and 4c KT2, respectively) for different geometries.

one-component PBE38 functional, those optimized with four-component PBE38 functional at the non-relativistic level and those derived from X-ray data). A small, but noticeable increase in the accuracy (about 3 ppm) was observed upon going from the non-relativistic equilibrium geometries to the effective geometries with taking into account relativistic effects. At the same time, the inclusion of relativistic effects at the stage of the calculation of chemical shifts demonstrates a significant decrease in the MAE by about 13 ppm, which is only 1.3% of the studied $^{15}$N NMR chemical shift range. A similar trend was also observed for the X-ray geometries with the MAE decreasing by about 4 ppm.

All the computations mentioned in the present work were performed using DIRAC[25] and DALTON[26] program codes.† Calculated shielding constants were converted into NMR chemical shifts scales according to the recommendations of IUPAC.[27]

In conclusion, a comparison between different computational approaches to the geometry optimizations and $^{1}$H, $^{15}$N and $^{195}$Pt NMR chemical shifts has been performed using cisplatin and transplatin as the model examples with known experimental data. The calculation of NMR chemical shifts in the non-relativistic approximation for the non-relativistic geometry did not allow us to reach practical results with any of the examined functionals, which is probably due to the fact that no relativistic effects were taken into account at this level. The accounting for these effects at the stage of the geometry optimization resulted in a small, but essential increase in the accuracy as compared to the non-relativistic geometries. A further and significant improvement in the accuracy can be achieved by including the relativistic effects at the full four-component relativistic level at the step of calculation of chemical shifts, which leads to the much smaller mean absolute errors. At this end, the relativistic effects allowed us to reach the accuracy as much as several hundreds of ppm for $^{195}$Pt NMR chemical shifts.

This work was supported by the Russian Foundation for Basic Research (grant no. 18-33-00334\18). All the calculations were performed at A. E. Favorsky Irkutsk Institute of Chemistry of the Siberian Branch of the Russian Academy of Sciences using computational facilities of the Baikal Analytical Center.

*Online Supplementary Materials*

Supplementary data associated with this article can be found in the online version at doi: 10.1016/j.mencom.2019.05.025.

† See Online Supplementary Materials for the computational details.

## References

1 S. P. A. *Sauer, Molecular Electromagnetism: A Computational Chemistry Approach*, University Press, Oxford, 2011.
2 T. Helgaker, M. Jaszuński and K. Ruud, *Chem. Rev.*, 1999, **99**, 293.
3 L. B. Krivdin, *Prog. Nucl. Magn. Reson. Spectrosc.*, 2017, **102**–**103**, 98.
4 L. B. Krivdin, *Prog. Nucl. Magn. Reson. Spectrosc.*, 2018, **105**, 54.
5 L. B. Krivdin, *Prog. Nucl. Magn. Reson. Spectrosc.*, 2018, **108**, 17.
6 Yu. Yu. Rusakov and L. B. Krivdin, *Russ. Chem. Rev.*, 2013, **82**, 99.
7 Y. Xiao, W. Liu and J. Autschbach, in *Handbook of Relativistic Quantum Chemistry*, ed. W. Liu, Springer, Berlin, 2017, pp. 657–697.
8 J. Autschbach, *Philos. Trans. R. Soc., A*, 2014, **372**, DOI: 10.1098/rsta.2012.0489.
9 J. Autschbach, in *High Resolution NMR Spectroscopy: Understanding Molecules and their Electronic Structures*, 1st edn., ed. R. H. Contreras, Elsevier, 2013, vol. 3, pp. 69–117.
10 M. Repisky, S. Komorovsky, R. Bast and K. Ruud, in *Gas Phase NMR*, eds. K. Jackowski and M. Jaszuński, Royal Society of Chemistry, Cambridge, 2016, pp. 267–303.
11 I. L. Rusakova, Yu. Yu. Rusakov and L. B. Krivdin, *Russ. Chem. Rev.*, 2016, **85**, 356.
12 I. L. Rusakova and L. B. Krivdin, *Mendeleev Commun.*, 2018, **28**, 1.
13 A. D. Becke, *J. Chem. Phys.*, 1993, **98**, 5648.
14 C. Lee, W. Yang and R. G. Parr, *Phys. Rev. B*, 1988, **37**, 785.
15 A. D. Becke, *J. Chem. Phys.*, 1993, **98**, 1372.
16 N. C. Handy and A. J. Cohen, *Mol. Phys.*, 2001, **99**, 403.
17 J. P. Perdew, K. Burke and M. Ernzerhof, *Phys. Rev. Lett.*, 1996, **77**, 3865.
18 C. Adamo and V. Barone, *J. Chem. Phys.*, 1999, **110**, 6158.
19 S. Grimme, J. Antony, S. Ehrlich and H. Krieg, *J. Chem. Phys.*, 2010, **132**, 154104.
20 D. H. Johnston, N. A. Miller and C. B. Tackett, *Acta Crystallogr., Sect. E: Struct. Rep. Online*, 2012, **68**, m863.
21 G. H. W. Milburn, M. R. Truter, M. Atoji, J. W. Richardson and R. E. Rundle, *J. Chem. Soc. A*, 1966, 1609.
22 T. W. Keal and D. J. Tozer, *J. Chem. Phys.*, 2003, **119**, 3015.
23 D. O. Samultsev, V. A. Semenov and L. B. Krivdin, *Magn. Reson. Chem.*, 2014, **52**, 222.
24 D. B. Chesnut and E. F. C. Byrd, *Chem. Phys.*, 1996, **213**, 153.
25 H. J. Aa. Jensen, R. Bast, T. Saue and L. Visscher, with contributions from V. Bakken, K. G. Dyall, S. Dubillard, U. Ekstroem, E. Eliav, T. Enevoldsen, E. Fasshauer, T. Fleig, O. Fossgaard, A. S. P. Gomes, T. Helgaker, J. Henriksson, M. Ilias, C. R. Jacob, S. Knecht, S. Komorovsky, O. Kullie, J. K. Laerdahl, C. V. Larsen, Y. S. Lee, H. S. Nataraj, M. K. Nayak, P. Norman, G. Olejniczak, J. Olsen, Y. C. Park, J. K. Pedersen, M. Pernpointner, R. Di Remigio, K. Ruud, P. Salek, B. Schimmelpfennig, J. Sikkema, A. J. Thorvaldsen, J. Thyssen, J. van Stralen, S. Villaume, O. Visser, T. Winther and S. Yamamoto, *DIRAC, A Relativistic Ab Initio Electronic Structure Program, Release DIRAC16*, 2016.
26 K. Aidas, C. Angeli, K. L. Bak, V. Bakken, R. Bast, L. Boman, O. Christiansen, R. Cimiraglia, S. Coriani, P. Dahle, E. K. Dalskov, U. Ekström, T. Enevoldsen, J. J. Eriksen, P. Ettenhuber, B. Fernández, L. Ferrighi, H. Fliegl, L. Frediani, K. Hald, A. Halkier, C. Hättig, H. Heiberg, T. Helgaker, A. C. Hennum, H. Hettema, E. Hjertenæs, S. Høst, I.-M. Høyvik, M. F. Iozzi, B. Jansik, H. J. Aa. Jensen, D. Jonsson, P. Jørgensen, J. Kauczor, S. Kirpekar, T. Kjærgaard, W. Klopper, S. Knecht, R. Kobayashi, H. Koch, J. Kongsted, A. Krapp, K. Kristensen, A. Ligabue, O. B. Lutnæs, J. I. Melo, K. V. Mikkelsen, R. H. Myhre, C. Neiss, C. B. Nielsen, P. Norman, J. Olsen, J. M. H. Olsen, A. Osted, M. J. Packer, F. Pawlowski, T. B. Pedersen, P. F. Provasi, S. Reine, Z. Rinkevicius, T. A. Ruden, K. Ruud, V. Rybkin, P. Salek, C. C. M. Samson, A. Sánchez de Merás, T. Saue, S. P. A. Sauer, B. Schimmelpfennig, K. Sneskov, A. H. Steindal, K. O. Sylvester-Hvid, P. R. Taylor, A. M. Teale, E. I. Tellgren, D. P. Tew, A. J. Thorvaldsen, L. Thøgersen, O. Vahtras, M. A. Watson, D. J. D. Wilson, M. Ziolkowski and H. Ågren, *WIREs Comput. Mol. Sci.*, 2014, **4**, 269.
27 R. K. Harris, E. D. Becker, S. M. Cabral de Menezes, P. Granger, R. E. Hoffman and K. W. Zilm, *Pure Appl. Chem.*, 2008, **80**, 59.

*Received: 29th October 2018; Com. 18/5727*